

Effects of laser frequency drift in phase-sensitive optical time-domain reflectometry fiber sensors

A.A. Zhirnov¹, A.K. Fedorov^{1,2}, K.V. Stepanov¹, E.T. Nesterov¹, V.E. Karasik¹, C. Svelto^{1,3}, and A.B. Pnev¹

¹*Bauman Moscow State Technical University, 2nd Baumanskaya St. 5, Moscow 105005, Russia*

²*Theoretical Department, DEPHAN, Novaya St. 100, Skolkovo, Moscow 143025, Russia*

³*Dipartimento di Elettronica e Informazione del Politecnico di Milano, Piazza Leonardo da Vinci 32, 20133 Milano, Italy*

(Dated: May 2, 2016)

The present work studies the influence of laser frequency drifts on operating of phase-sensitive optical time-domain reflectometry (Φ -OTDR) fiber sensors. A mathematical model and numerical simulations are employed to highlight the influence of frequency drifts of light sources on two characteristic scales: large-time (minutes) and short-time (milliseconds) frequency drifts. Numerical simulation results are compared with predictions given by the fluctuation ratio coefficient (FRC), and they are in a qualitative agreement. In addition to qualitative criteria for light sources given by the FRC, quantitative requirements for optimal light sources for Φ -OTDR sensors are obtained. Numerical simulation results are verified by comparison with experimental data for three significantly different types of light source.

I. INTRODUCTION

Distributed vibration sensors based on the Φ -OTDR technique are highly promising for remote control of long-distance objects such as bridges and pipelines [1]. In contrast to conventional OTDR sensing devices, probing the optic fiber with a narrowband light source allows locating perturbations by their effect on the backscattering signals (see Fig. 1), which are detected by taking into account their phases [2–4]. Last decades Φ -OTDR based sensing systems attracted a significant deal of interest [2–10]. Recent developments in manufacturing of fiber-optic components result in significant decrease of the production cost of such sensing devices.

However, phase-sensitive registration of backscattering light waves is possible only if the coherence length of the light source is not less than the pulse duration [2–9]. This requirement makes light sources one of the most expensive part of sensors. In general, quality of sensing systems for remote monitoring of extended objects is determined by its ability to detect perturbations caused by an activity near the sensor fiber within a background, where this background is formed both by external noises (*e.g.*, seismic noises) and self-noises of the system. In order to maximize the rate of recognized (*i.e.*, detected and classified) perturbations, Φ -OTDR based sensors have been studied throughout via numerical simulations [10–16].

A recent study [16] have shined a new light on the role of the laser source in Φ -OTDR based sensors. In particular, it has been demonstrated that a frequency drift of sources can suppress the signal-to-noise ratio (SNR) and even may cause failures. Numerical simulations based on calculating the FRC for different light sources take into account only the frequency drift on large-time scales (with respect to the characteristic operation time of Φ -OTDR systems, which is in order of milliseconds). This allows comparing a number of light sources and reveal the best one from this number. Thus, this method can be improved by development of quantitative criteria for laser sources for Φ -OTDR based sensors. One may also

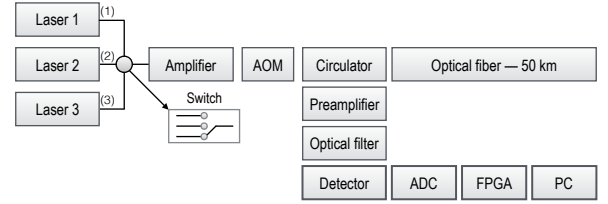


FIG. 1. Experimental setup: three types of laser (with different power, bandwidth, and frequency drift; AOM is acousto-optic modulator). The backscattering signal is launched into the detection part (bold line blocks): quadratic detector, analog-to-digital converter (ADC), field-programmable gate array (FPGA), and computer (PC). We also measure frequency drift of laser sources using highend wavemeter.

suppose that short-time scales are also important for operating of the Φ -OTDR based sensing systems since sufficiently fast frequency drifts can be a reason for failures.

In the present work, we study the effect of frequency drifts of laser sources for Φ -OTDR based sensing systems using experimental tests, numerical simulation, and experimental verification of the suggested model. First of all, we demonstrate experimentally the importance of frequency drift both on short-time and large-time scales by measuring the rate of correctly recognized in the background events for three light sources with different characteristics. On the basis of insights from experiment, we perform numerical simulation based on the mathematical model, which take into account two characteristic time scales of the frequency drift of laser sources. Thus, requirements for the frequency drift (additional to the once given by the FRC from Ref. [16]) for sources in Φ -OTDR based sensors, which aimed on maximization of the rate of correctly recognized events, are formulated.

Our paper is organized as follows. In Sec. II, we present experimental results on measurements of the rate of correctly recognized events for three light sources with different characteristics [18]. We emulate events by shock-like perturbation of fixed amplitude and fixed duration. Experimental insights on relation between the frequency

Sample	I , mW	$\Delta\nu$, kHz	l^{coh} , km	R_{det}	$\langle \text{FRC} \rangle_l$	$\nu(t)$, MHz/min	$\nu(t)$, MHz/20ms
1	10	0.5	600	0	2.27×10^6	40	25
2	10	5	60	0.75	2.63×10^5	40	0.5
3	10	7	44	1	2.06×10^5	2	0.3

TABLE I. Characteristics of three types of light sources used in our experiments [21]: power (I), linewidth ($\Delta\nu$), coherence length (l^{coh}), measured quantities of detection number, averaged fluctuation ratio coefficient (aFRC), as well as large-time and short-time scale frequency drifts (ν -drift).

drift shape of source and recognition rates forces us to include frequency drift behaviour in the mathematical model, which is described in Sec. III. We conclude and formulate additional criteria and quantitative requirements to laser sources for Φ -OTDR based sensing systems in Sec. IV.

II. EXPERIMENTAL TESTS

In order to obtain an insight about the role of the source frequency drift, we perform experimental measurements of the rate of correctly recognized events in the self-noises of the system with other background noises being negligible. We use the following experimental setup (see Fig. 1). A probe signal pulse from one of three laser sources, which are characterized by power (I), linewidth ($\Delta\nu$; with respect to time 20 ms), and coherence length (l^{coh}), is launched into the optical fiber (length of the fiber cable is about 25 km). These characteristics of investigated light sources are presented in Table I.

Backscattered waves of light are summed as amplitudes by taking into account their phases. Since they are randomly distributed, the measurement result is a randomly modulated signal. While the fiber is idle, the phases are not affected, and the shape of signals does not change. Any perturbation (event) near the optical fiber generates an acoustic wave that affects the fiber by displacement of scattering centers.

For each source, we create a set of test events by placing a source of shock-like impacts of fixed amplitude and duration near fixed point of the fiber cable. We measure simultaneously space-time intensity distributions formed by a set of sequentially measured signals.

Measured space-time field distribution $I(l, t)$ are input data for the filtering procedure based on the continuous wavelet transform of the following form

$$\mathcal{W}[a, b] = \int_{t=t_1}^T I(l, t) \psi_{a,b}(t) dt, \quad (1)$$

Here

$$\psi_{a,b}(t) \equiv \psi((t - b)/a), \quad (2)$$

a is the wavelet scale, b is the wavelet shift. For our signals, we use $a=10$, where ψ as the Symlets 8 wavelet function, which is near symmetric, orthogonal, and biorthogonal. After transform (1), we use exponential smoothing

filtering with the coefficient being equal to $\alpha_F = 0.05$. To detect an event in the background, we use the simple procedure based on calculation of exceeding the threshold I_c , which is highlighted by red lines in the Fig. 2. Also we note that such procedure is the basic step of the recognition algorithm for Φ -OTDR based sensors [22].

In our tests, we are primary interested in links between the rate R_{det} of correctly detected events, frequency drift behaviour, and parameters of the light source. We define the detection rate R_{det} in a straightforward way

$$R_{\text{det}} = \frac{N_{\text{correct}}}{N_{\text{total}}} - \frac{N_{\text{incorrect}}}{N_{\text{total}}}, \quad (3)$$

where N_{total} is the total number of events, N_{correct} is the number of correctly recognized events, and $N_{\text{incorrect}}$ is the number of incorrectly recognized events (failures). In fact, the R_{det} is the ratio of correctly detected perturbations to their total number during experiment with taking into account the number of incorrectly recognised events. During tests, N_{total} has order of tens events.

Field distributions for three laser sources are presented before and after filtering as well as results of measurements for frequency drifts for the sources during tests are presented in Fig. 2.

We start an analysis of our test from calculating of the FRC [16]. We calculate the mean value of the FRC for 10^2 counts the length of the sensor cable as follows

$$\langle \text{FRC} \rangle_l = \sum_{m=1}^L \left(\frac{1}{M_k - 1} \sum_{n=2}^{M_k} \frac{|I(l_m, t_n) - I(l_m, t)|}{\tau L} \right), \quad (4)$$

where L is the total number of length counts of the sensor cable, M_k is the total number of time counts during measurements, $I(l_m, t_n)$ is the registered intensity from m -th count of the cable in n -th count of time, and τ is the pulse duration.

Our results confirm influences of laser source instability predicted in Ref. [16]. The use of the FRC allows one to distinguish on the qualitative level that Sample (1) is worse than Sample (2) and Sample (3). Note that FRCs for Sample (2) and Sample (3) are close to each other. Thus, it is difficult to opt for Sample (3) demonstrating the best recognition rate by the FRC analysis only.

From results of our tests, presented in Table I and Fig. 2, we can conclude that Sample (3) has demonstrated the lowest frequency drift among tested laser sources (Fig. 2) and the highest recognition rate since all events are recognized in the background.

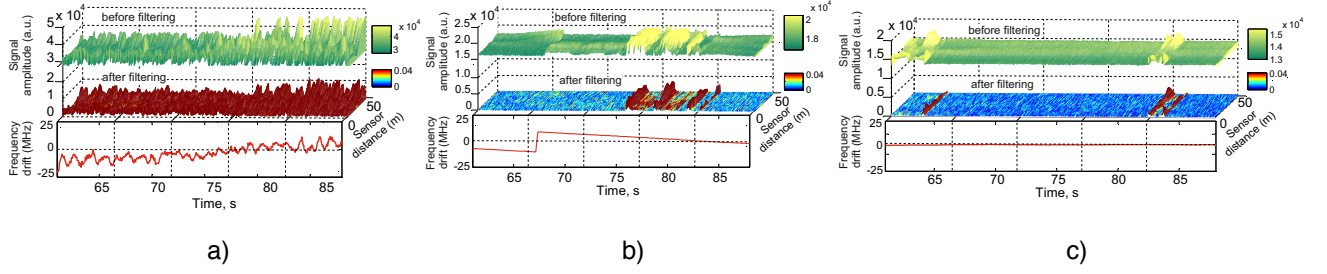


FIG. 2. The results of measurement of space-time field distribution $I(l, t)$ formed by a set of sequentially measured signals, the backscattering signal amplitude $I_l(t)$ in a particular point l as a function of time t , and the source frequency drift $\nu(t)$ are presented for three types of light source (temporal resolution of frequency drift measurements is 20 ms): (a)–(c) for the Sample (1), (d)–(f) for the Sample (2), (g)–(i) for the Sample (3). Experimental data clearly show that Sample (1) and Sample (2) with the same large-time scale behaviour demonstrate substantially different results of detection of test events in the background. Red ellipses contain test events during experiment.

Nevertheless, opting for Sample (3) is possible on analysis of both large-time and short-time scale frequency drifts. Sample with the lowest short-time scale frequency drift has the best results from the viewpoint of detection of external perturbations.

We note that Sample (1) has the narrowest linewidth. Counterintuitively, the Sample (1) has shown the worst results. But it instead shows much either short-term frequency drifts. The setup with this sample has not recognized a number of test events. Therefore, one can conclude that it is unsuitable for Φ -OTDR based sensors.

Sample (2) has demonstrated better results comparing Sample (1). Nevertheless, the setup with Sample (2) still was able to recognize all test events in the background. However, the frequency drifts region [see Fig. 2(b)] has become a reason for false alarms of the setup.

We also draw attention to the fact that measurements demonstrate that Sample (1) and Sample (2) with similar behaviour on large-time scale ($v_1(t) \approx 40$ MHz/min and $v_2(t) \approx 40$ MHz/min) show very different results of detection of test events in the background. However, these source have difference in short-time scale frequency drifts: $v_1(t) \approx 25$ MHz/20ms and $v_2(t) \approx 0.5$ MHz/20ms. Also, we point out on the fact that the Sample (3) demonstrating the best result has the lowest short-time scale drift: $v_2(t) \approx 0.3$ MHz/20ms. Combination of best characteristics on both time scales is crucial.

Thus, frequency changes on short-time scales are important from the viewpoint of detection of external perturbations. Therefore they should be taken into account on the path to formulation of quantitative requirements for optimal light sources for Φ -OTDR based sensing devices.

III. NUMERICAL SIMULATIONS

Insight from experimental data is that frequency drift on different time scales plays a crucial role for Φ -OTDR based sensing systems from viewpoint of recognition of events in the background noise. We describe a mathematical model accounting this peculiarity. By using this model, we simulate output signals for light sources with

different characteristics [18]. First, we verify our model by direct comparison of its prediction with the collected experimental data. After that, we compare different light sources from the viewpoint of registration of events in the background. Finally, the numerical result allows us to formulate quantitative criteria to select proper laser sources for Φ -OTDR based sensors, on the top of qualitative requirements given by FRC calculating [16].

The suggested impulse-response mathematical model is one dimensional. The model is based on the process of the detection of the optical signal after its interaction with scattering centers in the sensor fiber. The fiber is characterized by damping and dissipative factors. In turn, the light source can be characterized by the same parameters like in experiment (power, linewidth, and coherence length). The source power is important from the viewpoint of the SNR in the detection part of the sensor and generation of nonlinear effects in the sensor fiber [17]. The bandwidth of the signal and the coherence length define the maximal distance between the scattering center, which have an impact on the signal intensity. Finally, source frequency drifts are crucial for the SNR, and they are important both on short-time and large-time scales.

The suggested mathematical model is based on the fact that resulting signal after scattering on all centres can be viewed as a random complex-valued signal. We assume that the damping factor of the optical fiber is fixed on the level 0.17 dB/km. The scattering factor has more sophisticated structure. Then amplitude and phase distributions of scattering signals have the following Rayleigh form [13, 19]:

$$p(a) = \begin{cases} \frac{a}{\sigma^2} \exp\left[-\frac{a}{2\sigma^2}\right], & \text{if } a > 0, \\ 0, & \text{if } a < 0. \end{cases} \quad (5)$$

$$p(\phi) = \begin{cases} \frac{1}{2\pi}, & \text{if } \phi \in (-\pi, \pi], \\ 0, & \text{otherwise.} \end{cases}$$

We assume that amplitude a and phase ϕ of the signals are independent, where the set of amplitudes has the same distribution across the entire length of the sensor fiber and phases of the signal have a uniform distribution in the interval $(-\pi; \pi]$.

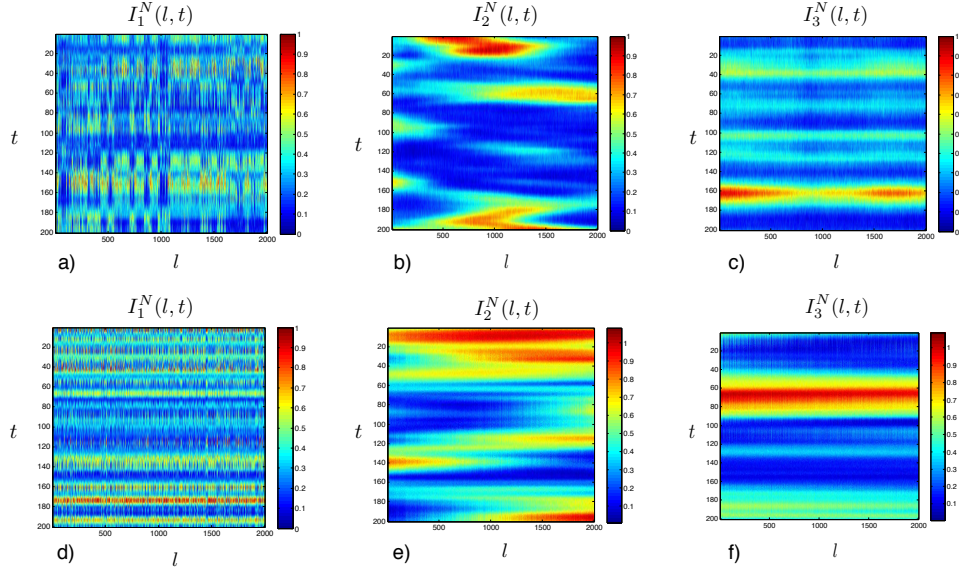


FIG. 3. Normalized space-time field distributions $I^N(l, t)$ for three types of laser sources [18]: comparison of experimental pictures [(a)–(c)] with results of numerical simulations [(d)–(f)].

The process of detection of signal can be described as an impulse–response model as follows. For a laser source with sufficiently narrow linewidth, the following expression holds for the backscattering intensity:

$$I(T) = I_0 \alpha(t) \left| \sum_{i_N} a_i \exp(-j\phi_i) \times \exp \left[\left(\frac{Tc/n - l_i}{l_{\text{coh}}} \right)^2 \right] \Theta \left(\frac{Tc/n - l_i}{l_{\text{imp}}} \right) \right|^2. \quad (6)$$

Here $I(T)$ is intensity of the signal before the detecting part (see Fig. 1), I_0 is the source power, i numerates scattering centers, a_i and ϕ_i are the scattering amplitude and phase of i -th center [they are distributed according to Eq. (5)], T is the travel time of signal, which can easily recalculated to the length as $z = Tc/n$, where n is the refractive index of the fiber, c is vacuum light speed, $\alpha(t)$ is the optical signal damping in the fiber, and $l_{\text{imp}} = \tau c/n$ is the pulse length in the fiber.

Assuming $l_{\text{coh}} \gg l_{\text{imp}}$, one can neglect temporal dependence of the exponential term in the square brackets:

$$\gamma \simeq \exp \left[\left(\frac{Tc/n - l_i}{l_{\text{coh}}} \right)^2 \right]. \quad (7)$$

Therefore, we transform (6) as follows

$$I(T) = I_0 \gamma \alpha(t) \left| \sum_{i=1}^N a_i \exp(-j\phi_i) \right|^2, \quad (8)$$

where N is the total number of scattering centers.

During the numerical simulations, we assume that the standard scattering center has the volume $200 \times 200 \times 200 \text{ nm}^3$ [23]. Therefore, the total number of scattering centers in the 10 m region of the fiber has the order of 10^{11} .

To reduce calculation time, we use the fact that sums of number with the Rayleigh distribution has the Rayleigh distribution. Then, one can approximate summation over $\sim 10^{11}$ scattering centers by calculation over $\sim 10^3$ scattering centers. Indeed, calculation of scattering phases of centers using the expression

$$\phi_i = 2\pi l_i / \lambda \quad (9)$$

is more efficient; λ is the laser wavelength.

One has to take into account filtering of the high-frequency part of the signal in the detecting part of the sensing system. Thus, we have

$$I_p(T) = I_0 \gamma \alpha(t) \left| \sum_{i=1}^N a_i \exp(-j\phi_i) \right|^2 \otimes \delta_{\text{det}}, \quad (10)$$

where δ_{det} is the detector impulse response (Fig. 1).

In this formalism, we can consider the process of formation of the response signal with respect to perturbations. A perturbation leads to displacements of scattering centers. Since the parameter l_j is changed for i -th scattering center, we should take into account resulting variation of the scattering phases. For simplicity, one can assume that variation of scattering centers can be described as follows:

$$\Delta l_i(t) = A \cos \left[\frac{2\pi(t - T_s)}{\tau_s} \right] \exp \left[-\frac{t - T_s}{\tau_a} \right], \quad (11)$$

where A is the perturbation amplitude, T_s is the time moment relation to the impact of the perturbation, τ_s is the period of perturbation induced oscillations, τ_a is the damping constant.

By substituting (11) to (9), we obtain periodical phase oscillations in the following form

$$\phi_i(t) = \frac{2\pi}{\lambda} [l_i + \Delta l_i(t)]. \quad (12)$$

Sample	$\langle STD \rangle_L^l$ exp	$\langle STD \rangle_L^l$ th	$\langle STD \rangle_L^s$ exp	$\langle STD \rangle_L^s$ th
1	0.1336	0.1188	0.1226	0.1175
2	0.1150	0.1043	0.0297	0.0313
3	0.0431	0.0424	0.0345	0.0360

TABLE II. Standard deviation calculated using Eq. (19) for long-term and short-term frequency drifts. Comparison of numerical simulations and experiments demonstrate very close results, which indicates on the correctness of the model.

This expression being substituted in Eq. (13) allows one to obtain the signal detected by the system in the case of absence of the background.

It should be noted that developed model assumes that the AOM creates perfect (in terms of zero-one amplitude) laser pulses. However, the AOM has the finite extinction ratio k_e being about 55 dB. Thus, this imperfection can be of interest for our system. Nevertheless, negative effects from this imperfection are not valid for the case, where the extinction ratio is much greater than the ratio between the length of the fiber and length of the pulse

$$k_e \gg l_{\text{fiber}}/l_{\text{pulse}}. \quad (13)$$

This is the case for our setup since k_e is about 55 dB and $l_{\text{fiber}}/l_{\text{pulse}}$ is close to 2500, *i.e.*, to 34 dB.

Second, we should take into account an additional impact position variations of the scattering centers due to thermal fluctuations, which can generally be described as a white noise in the following form

$$\phi_i(t) = \frac{2\pi}{\lambda} [l_i + \Delta l_i(t) + l_N(t)], \quad (14)$$

where $l_N(t)$ describes the position variation of the scattering centers.

Due to the frequency drift $\nu(t)$, one has:

$$\phi_i(t) = \frac{2\pi}{c} (\nu + \nu(t)) [l_i + l_N(t)]. \quad (15)$$

Here we distinguish two time scales:

$$\nu(t) = \nu_l(t) + \nu_s(t), \quad (16)$$

where $\nu_l(t)$ stands for large-time frequency drift (scales of minutes) and $\nu_s(t)$ stands for short-time frequency drift (scales of milliseconds).

In the detection part, there are additional sources of noise. They can be accounted as a white noise $N_p(t)$ as follows

$$I_p(t) = I_0 \gamma \alpha(t) \times \left| \sum_{i=1}^N a_i \exp(-j\phi_i(t)) \right|^2 \otimes \delta_{\text{det}} + N_p(t), \quad (17)$$

Considering all of these imperfections, we finally obtain

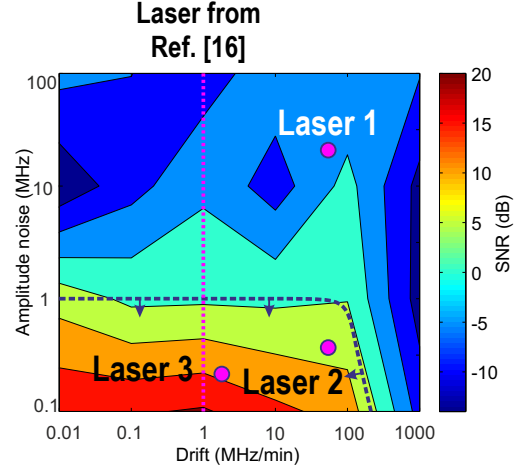


FIG. 4. Numerical simulations as quantitative results for optimizing an optimal light source for Φ -OTDR based sensing systems: circles stands for three studied sources, dotted line corresponds to a set of lasers chosen on the basis of criteria from Ref. [16], and dashed line highlights minimal requirements to the light source for Φ -OTDR sensors.

the following relation

$$I_p(t) = N_p(t) + I_0 \gamma \alpha(t) \times \left| \sum_{i=1}^N a_i \exp \left(-\frac{j2\pi}{c} [\nu + \nu_l(t) + \nu_s(t)] \times [l_i + l_N(t) + \Delta l_i(t)] \right) \right|^2 \otimes \delta_{\text{det}}. \quad (18)$$

Eq. (18) is the quintessence of the suggested mathematical model for Φ -OTDR sensing systems. This expression describes the signal $I_p(T)$ registered by the Φ -OTDR sensor in the time moment T . This signal consists of the noise component $N_p(t)$, which can be treated using the method described Ref. [17], and the useful signal.

Input data for Eq. (18) are signal power I_0 , coefficient γ (7) depending on coherent properties of the laser source, and the optical signal damping in the fiber $\alpha(t)$. Summation takes place over scattering centers. We point out that the important ingredient of this model is taking into account two time scales $\nu_l(t)$ and $\nu_s(t)$. The final expression should be also converged with the detector impulse response.

To obtain the signal without external perturbations, one can just set input data for the light source and put them into Eq. (18), chose configuration of scattering centers, distributions of amplitudes, and frequency drift on two scales. External perturbation described by the term $\Delta l_i(t)$ is zero. In order to obtain the result of measurements of Φ -OTDR sensing system with external perturbation, one need to set its amplitude and envelope similar to that in Eq. (11).

In order to verify the suggested model and its predictions, we compare the numerical results with experiments for our three laser sources. The results of simulations (see

Fig. 3) of the space-time field distribution $I(l, t)$ for three different lasers allow one to conclude that the model reproduces experimental pictures with sufficiently high precision.

Because of the random nature of optical signals, for estimation we use the following procedure. One can directly compare standard deviation of the signal from numerical simulation and experiments calculated as follows

$$\langle STD \rangle_L = \frac{1}{L} \sum_{i=1}^L \sqrt{\frac{1}{M_k} \sum_{k=1}^{M_k} [I(l_k, t_i) - \langle I(l_k, t) \rangle]^2}, \quad (19)$$

where the average value of the signal has been calculated according to the following expression:

$$\langle I(l_j, t) \rangle = \frac{1}{M_k} \sum_{k=1}^{M_k} I(l_j, t_k). \quad (20)$$

The detailed results in Table II. We present standard deviation calculated using Eq. (19) for long-term and short-term frequency drifts. Comparison of numerical

simulations and experiments demonstrate very close results, which indicates on the correctness of the model.

IV. DISCUSSIONS AND CONCLUSIONS

Now we also can formulate quintile criteria for the light source. Towards this end, we study the dependence between the number of properly revealed non-conventional events. On the basis of this study, we can conclude that the light source can have smooth drift of the center wavelength source up to 100 MHz/min, and short-term stability should be below the level 1 MHz. This is presented in Fig. 4.

ACKNOWLEDGEMENTS

We thank S. Nikitin for useful comments. This work was supported by the Ministry for Education and Science of the Russian Federation within the Federal Program under Contract No. 14.579.21.0104 (A.K.F.).

-
- [1] For a review, see X. Bao and L. Chen, *Sensors* **12**, 8601 (2012).
 - [2] H.F. Taylor and C.E. Lee, U.S. patent 5, 194847, March 16, 1993.
 - [3] J. Park, W. Lee, and H. F. Taylor, *Proc. SPIE* **3555**, 49 (1998).
 - [4] K.N. Choi and H.F. Taylor, *IEEE Photon. Technol. Lett.* **15**, 386 (2003).
 - [5] J.C. Juarez, E.W. Maier, K.N. Choi, and H.F. Taylor, *J. Lightwave Technol.* **23**, 2081 (2005).
 - [6] Y.J. Rao, J. Luo, Z.L. Ran, J.F. Yue, X.D. Luo, and Z. Zhou, *Proc. SPIE* **7503**, 75031O (2009).
 - [7] Y. Lu, T. Zhu, L. Chen, and X. Bao, *J. Lightwave Technol.* **27**, 3243 (2010).
 - [8] H.F. Martins, S. Martin-Lopez, P. Corredera, P. Salgado, O. Frazão, and M. González-Herráez, *Opt. Lett.* **38**, 872 (2013).
 - [9] H.F. Martins, S. Martin-Lopez, P. Corredera, M.L. Filograno, O. Frazão, and M. González-Herráez, *J. Lightwave Technol.* **31**, 3631 (2013).
 - [10] E.T. Nesterov, A.A. Zhirnov, K.V. Stepanov, A.B. Pnev, V.E. Karasik, Ya.A. Tezadov, E.V. Kondrashin, and A.B. Ushakov, *J. Phys. Conf. Ser.* **584**, 012028 (2015).
 - [11] A.E. Alekseev, Ya.A. Tezadov, and V.T. Potapov, *J. Commun. Tech. Electron.* **56**, 1490 (2011).
 - [12] A.E. Alekseev, Ya.A. Tezadov, and V.T. Potapov, *Quantum Electron.* **42**, 76 (2012).
 - [13] A.E. Alekseev, Ya.A. Tezadov, and V.T. Potapov, *Tech. Phys. Lett.* **38**, 89 (2012).
 - [14] Q. Li, C. Zhang, L. Li, and X. Zhong, *Optik* **125**, 2099–2103 (2014).
 - [15] L.B. Liokumovich, N.A. Ushakov, O.I. Kotov, M.A. Bisyarin, and A.H. Hartog, *J. Lightwave Technol.* **33**, 3660 (2015).
 - [16] X. Zhong, C. Zhang, L. Li, S. Liang, Q. Li, Q. Lü, X. Ding, and Q. Cao, *Appl. Opt.* **53**, 4645 (2014).
 - [17] A.B. Pnev, A.A. Zhirnov, K.V. Stepanov, E.T. Nesterov, D.A. Shelestov, and V.E. Karasik, *J. Phys. Conf. Ser.* **584**, 012016 (2015).
 - [18] Parameters of light sources used in experimental setups and simulations correspond to available on market lasers with the following values of the central frequency: for Sample (1) it is 193 490 GHz, for Sample (2) it is 193 460 GHz, and for Sample (3) it is 193 400 GHz.
 - [19] J.W. Goodman, *Statistical Optics* (Wiley-Interscience, New York, 1985).
 - [20] X. Chen, X. Zhang, B. Yan, J. Li, X. Chen, G. Tu, Y. Liang, Z. Ni, B. Culshaw, and F. Dong, *Proc. SPIE* **8421**, 8421A3 (2012).
 - [21] We note that the power of light pulse after the amplifier is about 300 mW.
 - [22] A.K. Fedorov, M.N. Anufriev, A.A. Zhirnov, K.V. Stepanov, E.T. Nesterov, D.E. Namiot, V.E. Karasik, and A.B. Pnev, *Rev. Sci. Instrum.* **87**, 036107 (2016).
 - [23] C.A. Bunge, R. Kruglov, and H. Poisel, *J. Lightwave Technol.* **24**, 3137 (2006).